

DEVELOPMENT AND DISEASE

PTEN is essential for cell migration but not for fate determination and tumourigenesis in the cerebellum

Silvia Marino^{1,†}, Paul Krimpenfort², Carly Leung¹, Hetty A. G. M. van der Korput³, Jan Trapman³, Isabelle Camenisch¹, Anton Berns² and Sebastian Brandner^{4,*†}

¹Institute of Pathology, University Hospital, 8091 Zurich, Switzerland

²Division of Molecular Genetics and Centre of Biomedical Genetics, The Netherlands Cancer Institute, CX 1066 Amsterdam, The Netherlands

³Department of Pathology, Erasmus University, 3000 DR Rotterdam, The Netherlands

⁴Institute of Neuropathology, University Hospital, 8091 Zurich, Switzerland

*Present address: Institute of Neurology, Queen Square, London WC1N 3BG, UK

†Authors for correspondence (e-mail: silvia.marino@pty.usz.ch or sebastian.brandner@prion.ucl.ac.uk)

Accepted 2 May 2002

SUMMARY

***PTEN* is a tumour suppressor gene involved in cell cycle control, apoptosis and mediation of adhesion and migration signalling. Germline mutations of *PTEN* in humans are associated with familial tumour syndromes, among them Cowden disease. Glioblastomas, highly malignant glial tumours of the central nervous system frequently show loss of *PTEN*. Recent reports have outlined some aspects of *PTEN* function in central nervous system development. Using a conditional gene disruption approach, we inactivated *Pten* in mice early during embryogenesis locally in a region specific fashion and later during postnatal**

development in a cell-specific manner, to study the role of *PTEN* in differentiation, migration and neoplastic transformation. We show that *PTEN* is required for the realisation of normal cerebellar architecture, for regulation of cell and organ size, and for proper neuronal and glial migration. However, *PTEN* is not required for cell differentiation and lack of *PTEN* is not sufficient to induce neoplastic transformation of neuronal or glial cells

Key words: *PTEN*, Cerebellum, *Cre-LoxP*, Lhermitte-Duclos Syndrome, Mouse

INTRODUCTION

The tumour suppressor gene *PTEN* encodes a lipid phosphatase, which has been shown to play a crucial role in the regulation of adhesion, migration, growth and apoptosis. *PTEN* germline mutations have been detected in several familial tumour syndromes, the most prominent of which are Cowden disease (CD) and Bannayan-Zonana (BZ) syndrome. These syndromes are characterised by developmental defects, benign tumours/hamartomas and a propensity to develop thyroid and breast cancer (Lloyd and Dennis, 1963). A subset of individuals with CD develops cerebellar gangliocytoma with abnormal and enlarged foliation caused by thickened and broadened layers of dysplastic and disorganised neuronal cells, also known as Lhermitte-Duclos disease (Lhermitte and Duclos, 1920). In addition to the disorganised cerebellar architecture, these individuals can show macrocephalia and mental retardation, and can develop seizures (Padberg et al., 1991).

However, although *PTEN* germline mutations have been demonstrated to be associated with CD and BZ syndromes, there is a considerable variability in genotype-phenotype

correlation in individuals with identified mutations, and large studies have failed to detect *PTEN* germ line mutations in all individuals with CD and BZ syndrome (Marsh et al., 1998a; Marsh et al., 1998b). The phenotypic variability of specific mutations suggests the involvement of further tumour modifier genes (Marsh et al., 1999).

Several studies have been undertaken to elucidate the role of *PTEN* during development and tumourigenesis of the central nervous system. First evidence for the importance of *PTEN* in developmental processes was provided by the analysis of *Pten*^{-/-} mice, which showed overgrowth of cells and disorganised cell layers in cephalic and caudal regions, resulting in early embryonic lethality (Di Cristofano et al., 1998; Podsypanina et al., 1999). *Pten*^{-/-} embryonic stem cells fail to form embryoid bodies in vitro and to differentiate when transplanted into recipient mice suggesting a crucial role of *PTEN* in the differentiation process (Di Cristofano et al., 1998; Podsypanina et al., 1999) and *Pten*^{-/-} embryos show an extensive proliferation and overgrowth (Stambolic et al., 1998).

Recently, cre loxP mediated inactivation of *Pten* in neural precursors during midgestation showed severe dysplasia with disturbance of the laminar organisation of the brain

incompatible with postnatal life. In vitro data however showed that *Pten*-deficient neural precursor cells have retained the capacity to differentiate into neurones, astrocytes and oligodendrocytes (Groszer et al., 2001) but it remains unclear whether and to what extent *Pten*-deficient neural stem cells are capable of attaining terminal differentiation in vivo. Instead, inactivation of *Pten* in cerebellar granule cells leads to progressive increase in cell size and to slight retardation of cell migration (Backman et al., 2001; Kwon et al., 2001).

Loss of heterozygosity of *P TEN* has been detected in many human cancers, mainly in endometrial and ovarian cancer, and in late stage metastatic tumours and glioblastoma, a malignant brain tumour (Li et al., 1997). Accordingly, mice chimaeric or heterozygous for *Pten* show an increased spontaneous tumour incidence (Di Cristofano et al., 1998; Podsypanina et al., 1999). Moreover, inactivation of just one *Pten* allele has been shown to increase proliferation and cell survival and to decrease apoptosis (Di Cristofano et al., 1999; Podsypanina et al., 1999). Therefore, *Pten* haploinsufficiency has been suggested as an important factor in early selection and expansion of cells during transformation (Di Cristofano and Pandolfi, 2000). We inactivated *Pten* at two different time points of cerebellar development in a region specific or cell specific fashion, to study the role of *Pten* in differentiation, migration and neoplastic transformation.

MATERIALS AND METHODS

Generation of *Pten* conditional mutant mice

Pten conditional mice were generated by introducing loxP recognition sequences into the fourth and the fifth intron of the *Pten* gene, flanking exon 5. A 9 kb fragment containing a neomycin selection cassette flanked by loxP sites and a *LoxP* sequence 1.3 kb downstream of Exon 5 (Fig. 1) was electroporated into ES cells. Southern blot analysis of targeted clones after homologous recombination was performed on *Bgl*III digested genomic DNA and probed with a ³²P-labelled exon 4 ('probe 1'). A 6.6 kb wild-type band (Fig. 1F, lanes 1-3) and a 5 kb band of the recombined allele (Fig. 1F, lane 1) were detected in a subset of clones. Probing with exon 5 ('probe 2') of *Nco*I/*Eco*RI-digested genomic DNA resulted in a 6 kb wild-type (Fig. 1G, lanes 1-3) and a 2 kb recombined band in these clones (Fig. 1G, lanes 1, 2). Southern blot analysis of *Nco*I/*Eco*RI-digested genomic DNA of selected clones after transient co-transfection with cre and puromycin expressing plasmids shows a 6 kb wild-type band (Fig. 1H, lanes 1-4) and a 2 kb floxed exon 5 band (Fig. 1H, lane 3) when probed with exon 5. Loss of the neo cassette was confirmed after re-probing the blot with a neo probe (Fig. 1H, lane 3). Mice carrying the *Pten* lox allele were derived by blastocyst microinjection.

Generation of L7cre transgenic mice

L7cre transgenic mice were generated by microinjection into male pronuclei of fertilised oocytes of FVB mice of a *Hind*III/*Eco*RI fragment containing a cre cDNA fragment cloned into exon 4 of the *L7* gene [kindly provided by Jim Morgan (Oberdick et al., 1990); Fig. 7A]. Expression patterns were determined by crossing the F₁ generation of *L7cre* mice with ROSA26 reporter mice (Soriano, 1999). Several mouse lines showed an expression restricted to Purkinje cells (see Fig. 7B-D), therefore line *L7cre*⁷⁵⁶ was used for all further experiments. Engrailed 2 transgenic mice (Zinyk et al., 1998) were kindly provided by Alexandra Joyner (Skirball Institute of Biomolecular Medicine, New York University School of Medicine).

Characterisation of mice

Genomic DNA was extracted from tail tips according to standard protocols and amplified with primers Cre1 (5'-ACC AGC CAG CTA TCA ACT C-3') and Cre2 (5'-TAT ACG CGT GCT AGC GAA GAT CTC CAT CTT CCA GCA G-3') yielding a 269 bp product. Thermocycling conditions consisted of 30 cycles of 30 seconds at 94°C, 30 seconds at 56°C and 50 seconds at 72°C. Reactions contained 200 ng template DNA, 0.5 μM primers, 100 μM dNTPs, 9% glycerol, 2.5 U Taq polymerase, 1.8 mM MgCl₂, 1×PCR buffer (Gibco-BRL) in a 20 μl volume.

ROSA 26R mice were screened by PCR using the same conditions described above and primers LZ1 (5'-CGT CAC ACT ACG TCT GAA CG-3') and LZ2 (5'-CGACCAGATGATCACACTCG-3'). Tail DNA from *Pten*^{LoxP} mice was amplified for 30 cycles (30 seconds at 94°C, 30 seconds at 62°C and 50 seconds at 72°C) using primers *Pten* A (5'-GGC AAA GAA TCT TGG TGT TAC-3') and *Pten* S (5'-GCC TTA CCT AGT AAA GCA AG-3'). The composition of the PCR mix was identical for all reactions.

Histology, immunohistochemistry and in situ hybridisation

For routine sections, brains were removed, immersion-fixed in 4% buffered paraformaldehyde for at least 4 hours, cut in coronal or sagittal planes and dehydrated through graded alcohols. After paraffin embedding, sections (3 μm) were cut and mounted on coated slides (Super Frost) and routinely stained with Haematoxylin and Eosin. The following antibodies or antisera were used for immunostaining: glial fibrillary acidic protein (GFAP, polyclonal antiserum 1:300, DAKO), S-100 (polyclonal rabbit antiserum, 1:2000, DAKO), synaptophysin (polyclonal antiserum 1:300; Zymed), microtubule-associated protein (MAP2, mouse monoclonal antibody 1:500; Roche), phosphorylated neurofilament protein (200 kDa subunit) (mouse monoclonal antibody 1:200, Sigma), neuronal nuclei (NeuN, mouse monoclonal 1:4000; Chemicon), parvalbumin (polyclonal rabbit antiserum, 1:750, SWANT), calbindin (polyclonal rabbit antiserum, 1:200, Chemicon), p27 (polyclonal rabbit antiserum 1:500, Santa Cruz), p-Akt (monoclonal mouse antibody 1:300, Cell Signalling Technology), phosphorylated histone H3 (polyclonal rabbit antiserum 1:1000, Upstate Biotechnology) and BrdU (monoclonal mouse antibody, 1:200, DAKO). A microwave pre-treatment for antigen unmasking was applied for synaptophysin, MAP2, NeuN, parvalbumin, calbindin, p27, p-Akt and BrdU. Detection was accomplished using biotinylated secondary antibodies, streptavidin-peroxidase complex and DAB. The automated NEXES immunohistochemistry machine (Ventana, Tucson, AZ) was used for all antibodies apart from p-Akt and p27.

In situ hybridisation for *Math1* (*Atoh1* - Mouse Genome Informatics) (probe was a gift from H. Zoghbi, HHMI, Baylor College of Medicine, Houston, TX), proteolipid protein and metabotropic glutamate receptor 2 (*mGluR2*) (probe from S. Nakanishi from Kyoto University, Japan) were carried out as described previously (Marino et al., 2000). The TSA amplification kit was used for *Math1* and *mGluR2*.

For in situ detection of apoptosis, the Roche TUNEL kit was used.

Immunoblotting

Cerebellar vermis from *L7cre*; *Pten*^{LoxP/LoxP}, *L7cre*; *Pten*^{LoxP/+}, *En2cre*; *Pten*^{LoxP/LoxP} and of wild-type mice was homogenised, and protein extracted in lysis buffer [1% NP 40, 150 mM NaCl, 50 mM Tris-HCl (pH 8.0), 0.1% SDS, 0.5% deoxycholic acid, 2 mM EDTA, Complete Protease Inhibitor Cocktail (Roche)] for 30 minutes at 4°C. Protein (30 μg) was resolved on 14% SDS-polyacrylamide gel, transferred to nitrocellulose membrane (Schleicher and Schuell) and probed with the following antibodies: phospho-AKT (polyclonal rabbit antiserum, 1:500, Cell Signaling Technology) and actin (1:500, rabbit polyclonal, Sigma). HRP-conjugated anti-goat secondary antibody was used at 1:5000 (Santa Cruz Biotechnology), and

blots were visualised using enhanced chemiluminescence (ECL, Amersham). In addition, Chemoluminescent Signals were detected and quantified with a Kodak gel documentation system.

Whole-mount *lacZ* staining

To visualise β -galactosidase activity in organs of reporter mice, tissue slices (2-4 mm) or sagittal cut brains were processed as described elsewhere (Benninger et al., 2000). Paraffin wax-embedded sections of *lacZ* pre-stained brain slices were cut (3 μ m) and counterstained with Nuclear Red or were further processed with standard immunohistochemical techniques using DAB as a chromogen (see above).

Image acquisition and analysis

Image acquisition was done with a JVC video camera (1360 \times 1024 pixels) attached to Zeiss Axioskop. Measurements of area or cell number were carried out with AnalySIS software (www.soft-imaging.de). For the calculation of areas, an image was captured at low-power magnification and further processed offline. Cells were marked and counted up by the software on the captured image.

RESULTS

Generation and characterisation of *En2cre*; *Pten^{LoxP/LoxP}* mice

Pten conditional mice were generated by flanking exon 5 with *LoxP* sites (Fig. 1A-I). The inserted mutation did not affect the function of the *Pten* gene and crossing these mice with *deleter* Cre mice (Schwenk et al., 1995) mimicked the phenotype of the conventional *Pten* knockout mice (data not shown).

To achieve inactivation of *Pten* in a region-specific fashion in the developing cerebellum, *Pten* conditional mutant mice were intercrossed with *engrailed 2* (*En2*) *cre* mice (line 22) (Zinyk et al., 1998). This line of *En2cre* transgenic mice expresses cre in a narrow dorsal domain in the midbrain-hindbrain junction around embryonic day 9.5 (Zinyk et al., 1998). Cells originating from this domain later populate the

medial region of the cerebellum, which largely corresponds to the vermis.

Embryonal analysis at day 15.5 (E15.5) of *En2cre*; *Pten^{LoxP/LoxP}* mice revealed a striking increase in the cell size of all precursor cells resulting in increased organ size of the cerebellar anlage (Fig. 2A,B). In addition to the above-mentioned findings, a complete lack of foliation was observed at postnatal day 1 in *En2cre*; *Pten^{LoxP/LoxP}* mice (Fig. 2E,F).

In mice older than three weeks, we observed ataxia, impairment of balance and reduction of overall activity. Gross inspection of their brains revealed a lack of foliation and enlargement of the cerebellar vermis (Fig. 3A,B), in keeping with the developmental findings. Histologically and immunohistochemically, all distinctive cell types of the mature cerebellum such as Purkinje cells (calbindin), granule cells (NeuN), stellate (parvalbumin) and basket cells (parvalbumin and neurofilament 200), Golgi cells (mGluR-2 in situ hybridisation) (Ohishi et al., 1993), Bergmann glia (GFAP and S-100) and oligodendrocytes (proteolipid protein in situ hybridisation) were represented and fully differentiated, indicating that PTEN is not required for fate determination and terminal differentiation in vivo. Instead, our experiments show that PTEN provides important cues for cells migration and positioning during development: in mature cerebella, the majority of Purkinje cells were clustered in an area above the fourth ventricle without recognisable orientation, suggesting an impairment of migration and positioning during development (Fig. 3D,K-O). However, several Purkinje cells migrated towards the cerebellar surface, randomly intermingled with granule cells and occasionally reached the surface. Mature granule cells, as identified by NeuN immunostaining, failed to form a proper layer, but were either loosely distributed throughout the deeper cerebellum (Fig. 3H) or failed to migrate inwards, resulting in mature granule cells within the molecular layer (Fig. 3J), in agreement to previous findings (Backman et al., 2001; Kwon et al., 2001). Likewise, Golgi cells (Fig. 4K,L), stellate and basket cells, as well as non

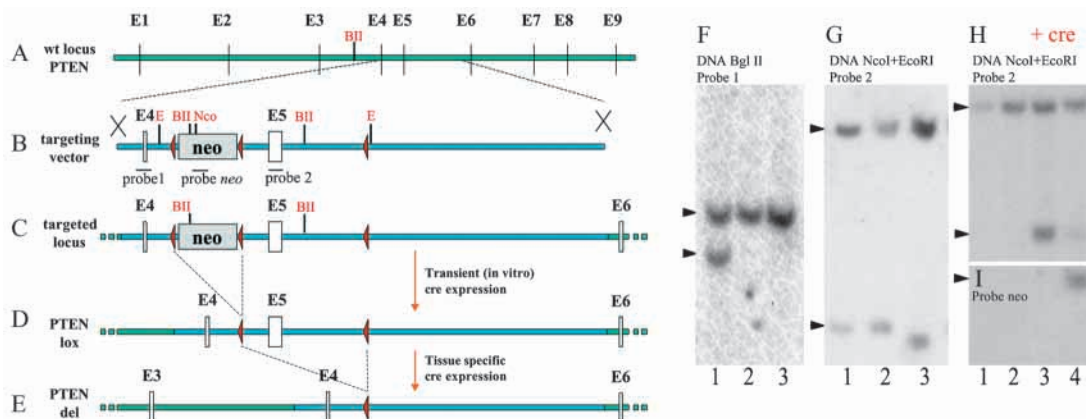


Fig. 1. Generation of mice deficient for PTEN in a tissue specific fashion: (A) organisation of the PTEN wild-type locus; (B) targeting construct used for electroporation into ES cells; (C) targeted locus containing the neomycin resistance gene flanked by *LoxP* sites; (D) ES cells lacking the neo cassette were generated by transient cre expression, resulting in a *Pten^{LoxP}* allele; (E) tissue-specific Cre-mediated recombination results in loss of exon 5. (F) Southern blot analysis of targeted clones after homologous recombination (*Bgl*II digest, probe 1; exon 4) shows a 6.6 kb wild-type band and a 5 kb band of the recombined allele in lane 1. (G) Probing with probe 2 (exon 5) of *Nco*I/*Eco*RI-digested genomic DNA resulted in a 6 kb wild-type and a 2 kb recombinant band in lanes 1+2. (H) Southern blot analysis (probe 2, *Nco*I/*Eco*RI-digested genomic DNA) after transient transfection with a Cre-expressing plasmid shows a 6 kb wild-type band and a 2 kb floxed exon 5 band. (lane 3). (I) Loss of the neo cassette was confirmed after re-probing the blot with a neo probe (lane 3).

neuronal cells (Bergmann glia and oligodendrocytes) (Fig. 4I,J), failed to assume proper position and rather were randomly distributed throughout the cerebellum. Ablation of only one *Pten* allele in *En2cre; Pten^{LoxP/wt}* mice did not result in abnormality of the cerebellum.

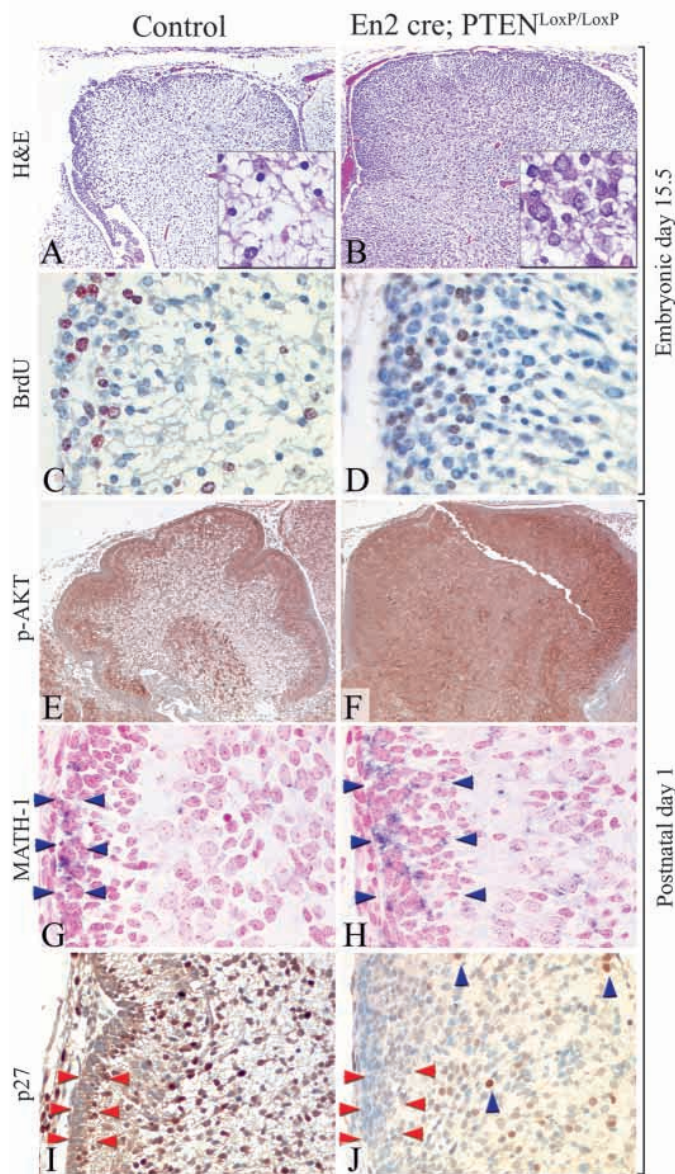


Fig. 2. Development, proliferation and differentiation in the cerebellum of *En2cre; Pten^{LoxP/LoxP}* mice. (A,B) enlarged cerebellar anlage and increased cell size (inset) of neural precursors at embryonic day 15.5 in *En2cre; Pten^{LoxP/LoxP}* (B) versus controls (A). (C,D) Immunostaining for BrdU revealed reduced proliferation in mutant cerebella at embryonic day 15.5 (D), compared with littermate controls (C). (E,F) Phosphorylated AKT is highly expressed in the EGL and IGL of the developing wild type cerebellum and in all regions of the mutant cerebellum. (G,I) Widening of the Math1-expressing outer EGL (G, arrowheads) and of the p27-expressing inner EGL (I, arrowheads). Littermate controls are shown in H and J; blue arrowheads in J indicate neurons strongly positive for p27. Scale bar: 400 µm in A,B (60 µm in inset); 50 µm in C,D; 660 µm in E,F; 100 µm in G,H; 200 µm in I,J.

No formation of tumours in *En2cre; Pten^{LoxP/LoxP}* mice

Loss of *Pten* has been described in a variety of malignant human tumours, including glioblastoma (Li et al., 1997; Wang et al., 1997). To assess, whether the lack of one or both alleles of *Pten* in mature neuronal or glial cells causes dysplasia or true neoplastic transformation, we kept 24 *En2cre; Pten^{LoxP/LoxP}* mice under observation for up to 28 weeks. Ataxic gait worsened between 3 and 8 weeks of age and remained steady thereafter. No additional sign of central nervous system damage appeared. Macroscopic examination of the brains confirmed enlargement and malformation of the vermis, as observed in younger animals. Moreover lateral or rostral displacement of the cerebellar hemispheres and of the occipital cortex respectively, was observed (Fig. 3A,B). Morphological analysis showed that dysplastic occasionally binucleated neurons (Fig. 3F, Fig. 4C,D), similar to those found in human cerebellar gangliocytoma, were already present in 7-week-old mice, whereas clearly dysplastic astrocytes (Fig. 4E) were detected after 16 weeks. However, no true neoplastic lesions were detected in these mice. This finding was in line with the lack of proliferating cells in the cerebellum of adult *En2cre; Pten^{LoxP/LoxP}* mice, as assessed by immunostaining for the proliferation marker p-histone H3 (data not shown). Our findings clearly demonstrate that lack of *Pten* is not sufficient to elicit neoplastic transformation neither in neuronal cells nor in glial cells. Surprisingly, Purkinje cells in *En2cre; Pten^{LoxP/LoxP}* mice (Fig. 4C) showed cytoplasmic accumulation of neurofilaments similar to tangles and exhibited vacuolation (Fig. 4C), both indicating progressive degeneration. Moreover, the overall number of Purkinje cells continuously decreased over time as shown schematically in Fig. 3K-O, where red dots indicate calbindin-positive Purkinje cells without overt signs of degeneration and green dots represent vacuolated, degenerating Purkinje cells. These findings suggest that the absence of *PTEN* in Purkinje cells leads to degeneration, rather than to neoplastic transformation.

Expression pattern of phosphorylated AKT and p27^{Kip1} in *En2cre; Pten^{LoxP/LoxP}* mice

Loss of *PTEN* leads to activation of the PI3K pathway and thereby to phosphorylation and activation of Akt (reviewed by Cantley and Neel, 1999). To investigate whether and to what extent activation of Akt is implicated in neuronal and glial abnormalities observed we set out to characterise the expression pattern of phospho Akt (p-Akt) in wild type and compound mutant mice using a p-Akt-specific antibody (Backman et al., 2001; Kwon et al., 2001).

To define the baseline of p-Akt expression in the developing and mature cerebellum, we performed immunohistochemical staining on wild-type brains at various time points. While p-Akt was strongly expressed in Purkinje cells and in granule cell precursors during development (Fig. 2E), a less intense p-Akt expression was noted in Bergmann glia cells and to lesser extent Purkinje cells and Golgi cells in the adult brain. In mutant *En2cre; Pten^{LoxP/LoxP}* cerebella at postnatal day 1, we detected a widespread expression of p-Akt, as expected from the architectural abnormalities (Fig. 2).

Interestingly, in adult cerebella of *En2cre; Pten^{LoxP/LoxP}* mice, strong p-Akt overexpression was observed in a fraction of dysplastic Purkinje cells (data not shown) and in the

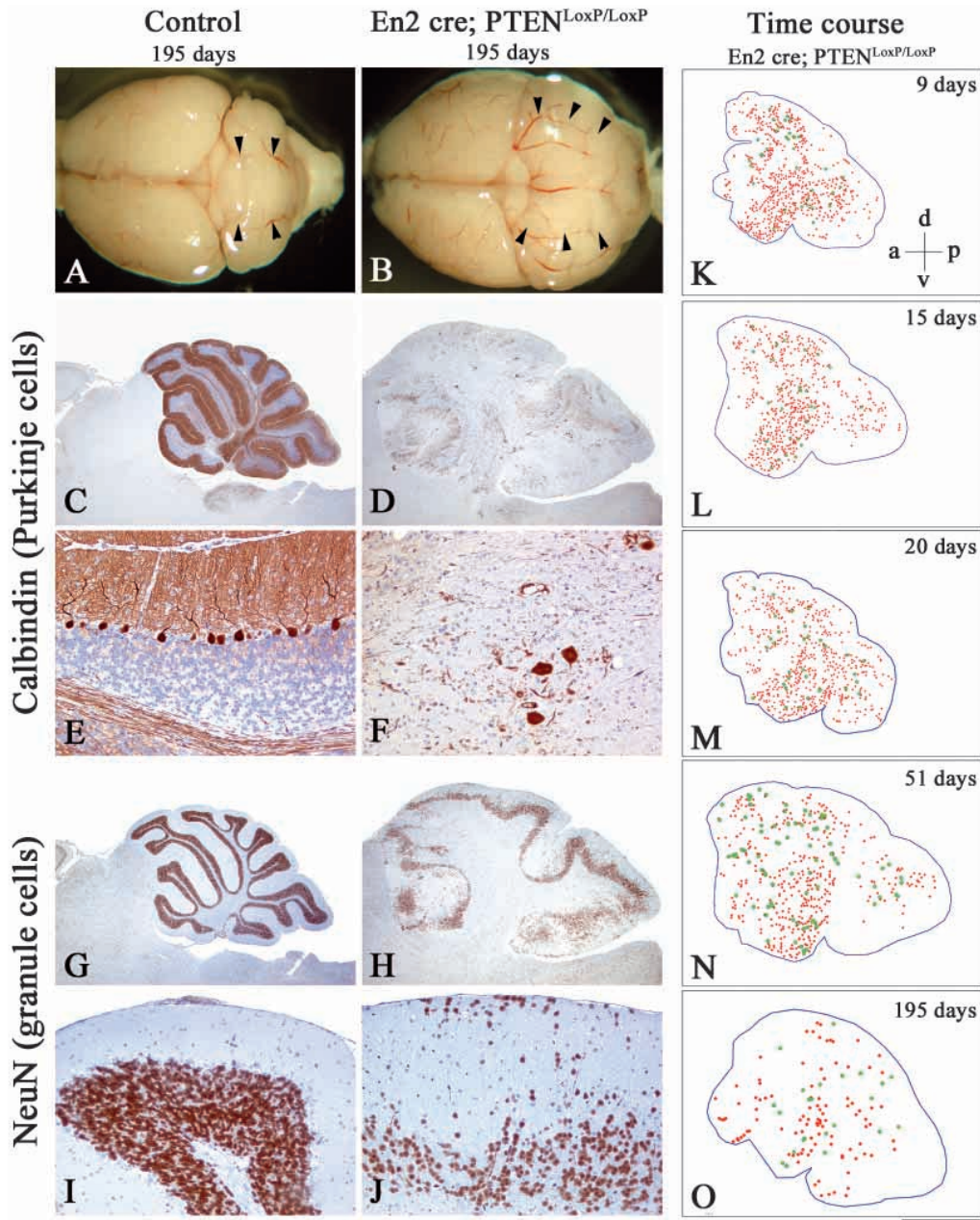


Fig. 3. Analysis of *En2cre*; *Pten*^{LoxP/LoxP} mice. (A,B) Significant enlargement of the cerebellar vermis of conditional mutant mice (195 days old) (B) when compared with age-matched controls (A). Arrowheads indicate the lateral extension of the vermis (A,B). (D,H) Sagittal sections revealed a significant increase in size of the cerebellum and loss of foliation. (C-F) Calbindin-positive Purkinje cells in mutant cerebellar areas were randomly distributed, enlarged and occasionally vacuolated (D,F) when compared with control littermates (C,E). Likewise, NeuN-positive granule cells were positioned parallel to the outer margin of the mutated cerebellum (H) and occasionally retained within the presumed molecular layer (J). Control brains are shown in G,I. Schematic illustration of the progressive loss of Purkinje cells over time (K-O): outline of the mid-sagittal cerebellum, each red dot represents one vital Purkinje cell on a representative midsagittal cerebellar section. Green dots represent vacuolated Purkinje cells in the same section. The orientation of the sections is indicated in K (a, anterior; p, posterior; d, dorsal; v, ventral). The age of the respective animals is indicated in each section. A digitised image and AnalySIS software were used to outline the section and to label vital or vacuolated Purkinje cells on a calbindin-stained slide. Scale bar: 2 mm in C,D,G,H; 100 μ m in E,F,I,J; 1.8 mm in K-O.

majority of dysplastic and non-dysplastic astrocytes (Fig. 4F). A weaker expression of p-Akt was detected in all other cell types of the cerebellar vermis, which, however, still exceeded the levels in PTEN-expressing cells. In keeping with these findings, immunoblotting of dissected vermis extracts of *En2cre*; *Pten*^{LoxP/LoxP} mice showed higher levels of p-Akt than the corresponding wild-type tissue (Fig. 5).

Akt activation affects cell cycle progression through inhibition of p27^{Kip1} protein levels. Phosphorylation of p27^{Kip1} by Akt results in its cytoplasmic retention and loss of its growth inhibition. As predicted, p27^{Kip1} expression levels inversely correlated with those of p-Akt in wild type as well as in mutant cells in the developing cerebellum. However, it should be noted that p27^{Kip1} levels in adult *En2cre*; *Pten*^{LoxP/LoxP} mice did not show a noticeable decrease compared to PTEN-expressing cells in laterally adjacent cerebellar regions. This finding is

confirmed by immunoblotting for p27 of the vermis of adult *En2cre*; *Pten*^{LoxP/LoxP} mice, which showed no difference from wild-type mice (data not shown).

The thickness of the external granule layer (EGL) during early postnatal development was increased (six or seven cells instead of four or five cells in thickness) in *En2cre*; *Pten*^{LoxP/LoxP} mice (Fig. 2G,H). To evaluate whether these cells were undifferentiated precursors that were still proliferating or whether they were already terminally differentiated but non-migrating granule cells, we performed mRNA in situ hybridisation for *Math1*, a marker of cerebellar granule cell progenitors (Ben-Arie et al., 2000; Helms and Johnson, 1998). We show that a considerable proportion of cells in the thickened EGL of mutant mice are *Math1* positive and therefore represent undifferentiated, still actively proliferating, granule cell progenitors.

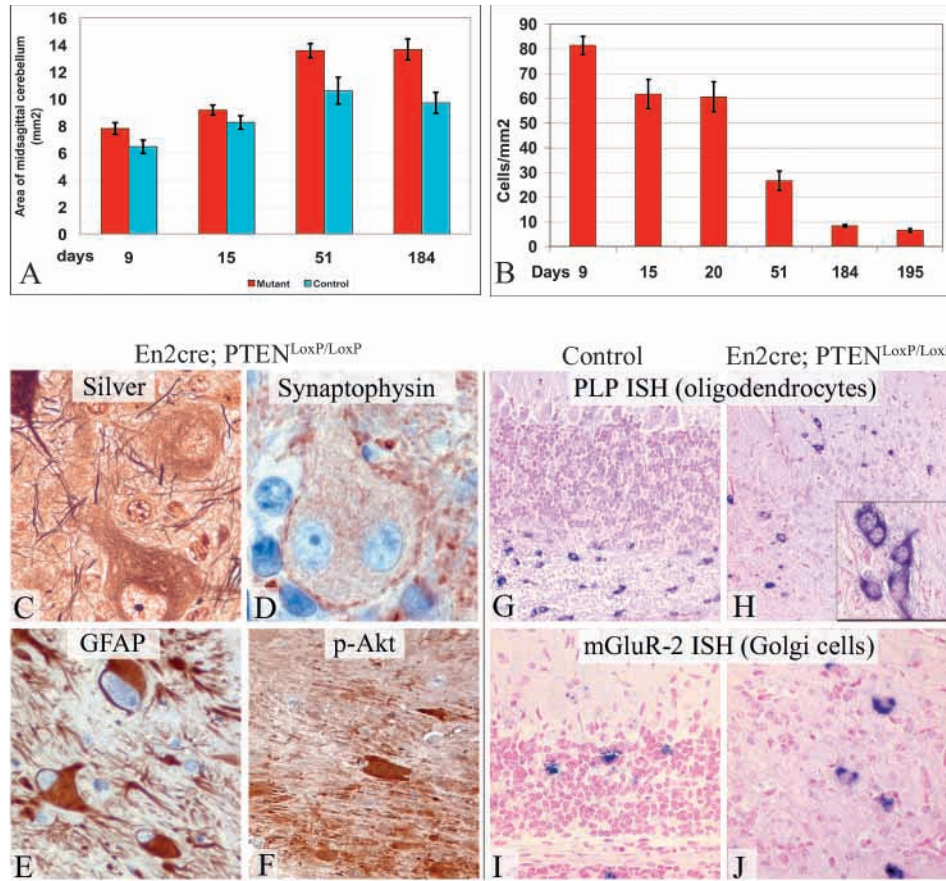


Fig. 4. Characterisation of pathological features in cerebella *En2cre*; *Pten^{LoxP/LoxP}* mice. (A) Increased cerebellar size expressed as midsagittal area (mm²) in mutant (red bars) versus controls (blue bars). Evaluation of three sections each. Vertical bars indicate s.d. Significance of the size difference: 9 days, $P < 0.03$; 15 days, $P < 0.02$; 51 days, $P < 0.004$; 184 days, $P < 0.01$. (B) Graphic representation of chronic Purkinje cell loss in *En2cre*; *Pten^{LoxP/LoxP}* mice expressed as cells per mm² in midsagittal sections stained for calbindin. Error bars indicate s.d. (C) Abnormal accumulation of neurofilaments in Purkinje cells *En2cre*; *Pten^{LoxP/LoxP}* mice visualised by Bielschowsky silver impregnation. (D) Occasionally, bi-nucleated neurones were encountered (synaptophysin immunostaining). (E,F) Dysplastic astrocytes, revealed by GFAP immunostaining (E) were seen in aged *En2cre*; *Pten^{LoxP/LoxP}* mice and showed heavy accumulation of phospho-AKT (F). (G,H) Oligodendrocytes (visualised by proteolipid protein in situ hybridisation) were mainly confined to the white matter tracts and only occasionally present within the granular or molecular layer in controls (G), while *En2cre*; *Pten^{LoxP/LoxP}* mutant mice (H) showed a random distribution of these

cells, which occasionally reached the cerebellar surface. Frequently, oligodendrocytes formed pairs or clusters (inset in H; I). (I,J) In situ hybridisation of metabotropic glutamate receptor 2 (mGluR2) reveals Golgi cells (cerebellum of control mouse, I) and showed abnormal positioning but no depletion throughout lifetime in *En2cre*; *Pten^{LoxP/LoxP}* mutant cerebella (J). Scale bar: 50 μ m in C,E; 30 μ m in D; 110 μ m in F-H; 80 μ m in I,J.

Cerebellar granule cell proliferation is controlled by p27^{Kip1} during development and p27^{Kip1} accumulates in EGL cells shortly before exit from cell cycle and terminal differentiation (Miyazawa et al., 2000). EGL cells in *En2cre*; *Pten^{LoxP/LoxP}* mice show a significantly decreased expression of p27^{Kip1} (Fig. 2I,J). Therefore, activation of Akt and downregulation of p27^{Kip1} may explain retarded maturation of PTEN deficient EGL cells.

Cell proliferation and cell death in the cerebellum of *En2cre*; *Pten^{LoxP/LoxP}* mice

Several studies have suggested that PTEN negatively regulates cell growth, and in vitro experiments suggest an increased proliferative potential of *Pten^{-/-}* neural stem cells (Groszer et al., 2001). We therefore examined cell proliferation at various time points during development using either or BrdU incorporation (Fig. 2C,D) or antibodies against phosphorylated histone H3, which is expressed during M-phase when the chromosomes are fully condensed. Surprisingly, both BrdU and phospho-histone H3 immunostaining showed less proliferation in *Pten*-deficient cerebella than in wild-type brains. Both the absolute number (i.e. labelled nuclei within the entire sagittal area of the cerebellum) and the relative number (i.e. labelled nuclei as a ratio of all nuclei) were reduced by a factor of two to three at E15.5, P1 and P9 in *Pten*-

deficient cerebella (Fig. 6F). To determine, whether increased size of cerebella in *En2cre*; *Pten^{LoxP/LoxP}* mice was caused by augmented cell numbers, increased cell size or both, we calculated cell numbers and cell density from sagittal sections. Surprisingly, overall cell density (i.e. the cell density of an entire sagittal section) was lower in *Pten* mutant cerebella at E15.5 and P1 (Fig. 6A), probably owing to the lower cellular density of the EGL in mutant animals. However, as the midsagittal area (Fig. 6B) was up to almost twofold larger in mutant cerebella, the absolute cell number was higher in mutant than in wild-type brains (Fig. 6C). TUNEL staining performed on E15.5 and P1 revealed a decreased apoptotic rate in the mutant cerebellum (Fig. 6D). Therefore, the decreased proliferation (Fig. 6F) is 'compensated' by a decreased cell death rate, which may explain why similar cell numbers are counted at postnatal day 1 (Fig. 6C).

Generation and characterisation of *L7 cre* transgenic mice

To analyse whether and to what extent migration disturbance, increased cell size and degeneration of Purkinje cells are cell autonomous, rather than a consequence of improper positioning and environment, we set out to inactivate *Pten* selectively in these cells. To this end, transgenic mice were generated in which Cre was expressed under the control of the

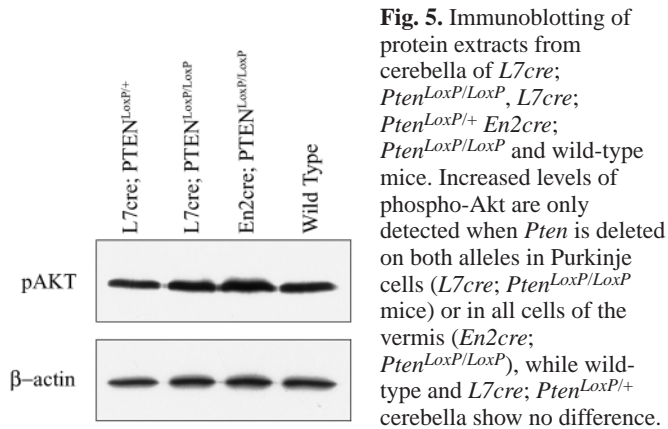


Fig. 5. Immunoblotting of protein extracts from cerebella of *L7cre*; *Pten*^{LoxP/LoxP}, *L7cre*; *Pten*^{LoxP/LoxP}, *L7cre*; *Pten*^{LoxP/LoxP} *En2cre*; *Pten*^{LoxP/LoxP} and wild-type mice. Increased levels of phospho-Akt are only detected when *Pten* is deleted on both alleles in Purkinje cells (*L7cre*; *Pten*^{LoxP/LoxP} mice) or in all cells of the vermis (*En2cre*; *Pten*^{LoxP/LoxP}), while wild-type and *L7cre*; *Pten*^{LoxP/LoxP} cerebella show no difference.

L7 promoter, which is mainly expressed in Purkinje cells (Oberdick et al., 1990). Progeny resulting from the pronuclear injection of the *L7cre* construct (Fig. 7A) were screened for integration of the transgene. Transgenic lines were derived from all 11 founder mice (FVB inbred). To investigate the tissue-specific expression and the functionality of the transgene two lines, Tg 753 and Tg 756, were crossed to ROSA26R indicator mice (Soriano, 1999). In situ enzymatic staining for β-galactosidase on brains of adult double transgenic mice revealed staining exclusively in Purkinje cells (Fig. 6B-D). No *lacZ* expression was detected outside the brain.

While *L7cre*; *Pten*^{LoxP/wt} mice showed no cerebellar abnormality, *L7cre*; *Pten*^{LoxP/LoxP} mice exhibited subtle irregularities of Purkinje cell lining but no major architectural disturbances and no clinical phenotype up to 20 weeks of age. All Purkinje cells showed noticeable increase in cell size, including thickening of dendrites and descending axons (Fig. 7E,F), while neighbouring cells (granule cells and Bergmann glia) remained unaffected. At later time points (17 and 20 weeks) Purkinje cells showed signs of degeneration (Fig. 6G) and cell loss, while there was no noticeable loss of granule cells. These experiments indicate that regulation of cell size depends on PTEN. Moreover loss of PTEN results in Purkinje cell degeneration in a cell-autonomous fashion. Immunohistochemical detection of phosphorylated Akt showed significantly higher p-Akt levels in Purkinje cells (Fig. 7I,J) than in wild-type animals (Fig. 6H). The accumulation of p-Akt was confirmed by immunoblotting of vermis extracts, showing a signal of intermediate intensity between wild-type and *En2cre*; *Pten*^{LoxP/LoxP} mice (Fig. 6). This is explained by the 'admixture' of granule cells that are not overexpressing p-Akt and therefore dilute down the intensity of p-Akt, while the vermis of *En2cre*; *Pten*^{LoxP/LoxP} mice contains almost exclusively *Pten* negative cells, resulting in a stronger p-Akt signal. Consistent with the lack of morphological signs of degeneration, increase of size or accumulation of p-Akt in Purkinje cells of *L7cre*; *Pten*^{LoxP/+} mice, immunoblotting revealed no difference from wild-type mice.

DISCUSSION

We inactivated *Pten* during embryonic development in all neuronal and glial cell populations in a precisely defined area

of the CNS (the cerebellum). This was achieved by using *En2cre* transgenic mice, in which cre is active in a narrow dorsal domain in the midbrain-hindbrain junction with a peak expression at embryonic day 9.5 (Zinyk et al., 1998). Cells originating from this domain later populate the medial region of the cerebellum, which corresponds reasonably well to the vermis.

This experimental approach allowed us to study the role of PTEN in cell migration and determination of cytoarchitecture during development. Moreover, as inactivation of *Pten* was restricted to a specific brain area, we did not elicit a lethal phenotype and therefore the differentiation potential of progenitor cells lacking *Pten* could be analysed.

We show here that PTEN is essential for cell migration and determination of lamination of the cerebellum. These results are consistent with the data obtained by inactivation of *Pten* in neural precursors during midgestation by nestin-mediated cre expression (Groszer et al., 2001). We observed that Purkinje cells were retained in large clusters above the fourth ventricle instead of migrating towards the cerebellar surface (Fig. 3K-O). As PTEN contributes to the regulation of cell adhesion and migration through the MAP kinase/focal adhesion kinases and Shk cascade (Tamura et al., 1999a; Tamura et al., 1998; Tamura et al., 1999b), impaired cell migration and positioning might be a consequence of defective adhesion signalling. It is possible, that impaired migration is due to a deregulated activity of phosphatidylinositol-3-kinase (PI3K). Ming et al. (Ming et al., 1999) have shown that nerve growth cone guidance is mediated by PI3K and there is evidence for an involvement of PI3K in cell migration (Jimenez et al., 2000; Shen and Guan, 2001). However, it has yet to be clarified to what extent the observed migration defect is cell autonomous (i.e. directly caused by *Pten* deficiency of the migrating cell) or rather indirectly a result of, for example, disturbed radial glia formation, which no longer provide guidance for migrating granule cells.

To date, it is unclear whether *Pten* plays a role in cell fate determination and terminal differentiation. So far the differentiation capacity of *Pten*-deficient neural precursor cells into astrocytic, oligodendroglial and neuronal lineages has been shown only in vitro (Groszer et al., 2001). The early postnatal lethality of *Nestin-Cre*; *Pten*^{LoxP/LoxP} mice precluded further analysis. Inactivation of *Pten* in already committed neuronal populations during postnatal development (Backman et al., 2001; Kwon et al., 2001), although compatible with postnatal life, does not allow us to address this point. Our data demonstrate for the first time that absence of *Pten* does not impair the capacity of neural progenitors to differentiate into all cell types of the mature cerebellum in vivo.

A surprising finding was the reduced fraction of proliferating cells in cerebella of *En2cre*; *Pten*^{LoxP/LoxP} mice during embryonic and early postnatal development. The proliferation was assessed with an antibody against phosphorylated histone H3, which labels nuclei during the M phase and confirmed by BrdU labelling at E15.5. These findings appear to be in disagreement with previous studies, in which proliferation was increased in *Pten*-deficient E14 neural sphere cultures and in the ventricular zone of *Nestin-cre*; *Pten*^{LoxP/Δ5} E14.5 embryos (Groszer et al., 2001). When BrdU-positive nuclei were related to the number of all (labelled and unlabelled) nuclei of the entire cerebellar section, a proliferation fraction of 12% was

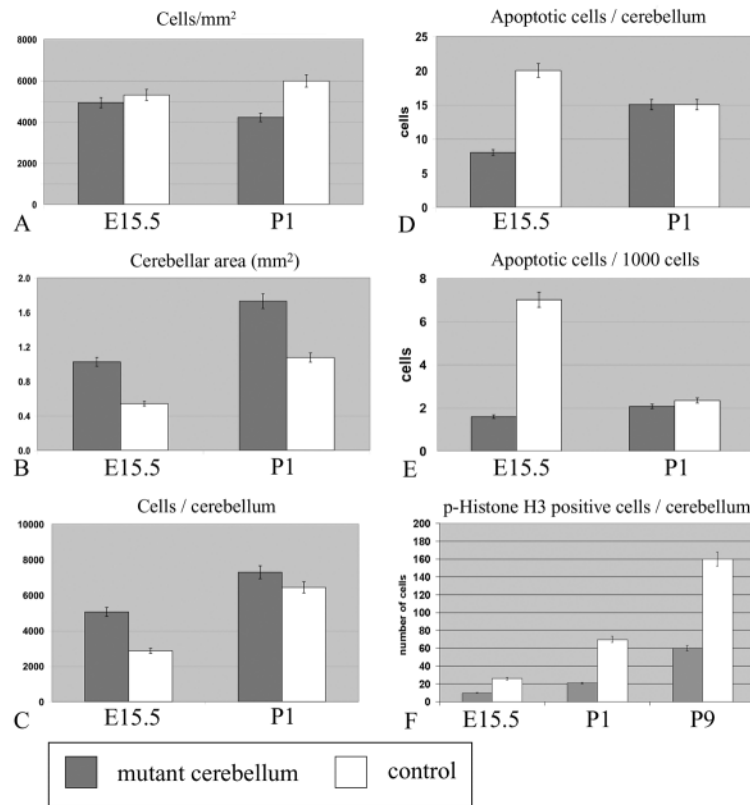


Fig. 6. Cell density, apoptosis and proliferation in the developing cerebellum of *En2cre; Pten^{LoxP/LoxP}* mice and controls at E15.5 and postnatally (P1). Although cellular density is not greatly increased at E15.5 (A), the absolute number of cells (C) in the midsagittal cerebellum is almost twice as much in mutant brains, because the total area is increased in mutants (B). Apoptosis is reduced in E15.5 mutant cerebella, compared with controls (D,E), but there is also reduced proliferation in mutant cerebella at days E15.5, P1 and P9 (F) in mutant versus control cerebella.

calculated in mutant versus 24% in wild-type cerebella at E15.5. Moreover, the number of p-histone H3 positive cells was considerably lower at E15.5, P1 and P9 in mutant compared with wild-type brains. There may be several reasons for the apparent discrepancy: (1) *Pten*^{-/-} neural stem cells grown in vitro may behave differently, as they are subjected to different environmental cues such as growth factor concentrations; and (2) it is possible that cerebellar precursor cells behave differently from neural precursor located in the ventricular zone. Moreover, it is possible that the reduced proliferation of the cerebellar precursor cells in our *Pten* mutant is a secondary effect, e.g. due to improper growth factor signalling in the disorganised cerebellum.

Inactivation of *Pten* later during CNS development did not result in a noticeable proliferation difference between mutant brains and controls after P10 (Backman et al., 2001; Kwon et al., 2001), perhaps because *Pten* was inactivated at a time point when the major fraction of precursor cells was already postmitotic and committed.

Inactivation of *Pten* results in activation of the PI3K/Akt pathway, which leads to subsequent phosphorylation and cytoplasmic retention and degradation of the cell cycle inhibitor p27. In accordance with this known effect of Akt, we

observed a decreased expression of p27 in the broadened EGL in *En2cre; Pten^{LoxP/LoxP}* mice and only single cells that had migrated inwards expressed p27 at higher levels (Fig. 2I,J). The marked increase in thickness of the EGL shows striking resemblance with the phenotype of *p27*^{-/-} (Cdkn1b – Mouse Genome Informatics) mice. However, although *p27*^{-/-} granule cell precursors show increased proliferation when compared with wild-type cells in vitro (Miyazawa et al., 2000), their proliferation rate in vivo has not yet been sufficiently addressed. Downregulation of p27 expression in EGL precursor cells of *En2cre; Pten^{LoxP/LoxP}* mice might be responsible for many of the effects observed. It has been proposed that p27 acts as a timer in precursor cell division in a dose-dependent fashion (Durand and Raff, 2000). Insufficient levels of p27 in EGL precursors may impair both cell cycle exit and differentiation. In agreement with this interpretation is the prolonged expression of the transcription factor *Math1*, member of neural basic helix-loop-helix factors controlling neural differentiation. Although expression of p27 in the EGL is generally taken as an indicator for cell cycle exit of inwards migrating precursor cells, the normally organised, though slightly enlarged, cerebellum of *p27*^{-/-} mice proves that alternate pathways are providing appropriate signals for cell cycle exit, differentiation and migration in *p27*^{-/-} mice.

A striking feature in *En2cre; Pten^{LoxP/LoxP}* mice was the chronic progressive loss of Purkinje cells (Fig. 3K-O), which started during early postnatal development and was characterised by vacuolation and accumulation of fibrillary inclusions (Fig. 4C). To analyse whether and to what extent increased cell size and degeneration of Purkinje cells are cell autonomous or whether this is a consequence of improper positioning and environment, we have generated *L7cre* mice to inactivate *Pten* selectively in Purkinje cells. *L7cre; Pten^{LoxP/LoxP}* mice exhibited similar features of Purkinje cell degeneration as *En2cre; Pten^{LoxP/LoxP}* mice (Fig. 7F,G). We therefore conclude that these effects are likely to be cell autonomous, rather than a consequence of improper migration or micro-environment. Degenerative changes followed by cell loss noted for Purkinje cells point to a possible role of *Pten* and its downstream targets, in neurodegeneration. However, it is not clear how the observed cell death is brought about, as several studies suggest a role of Akt in promoting cell survival rather than triggering degeneration (Eves et al., 1998; Gary and Mattson, 2001; Tanno et al., 2001; Zhou et al., 2001). However, these findings were obtained in growing rather than in terminally differentiated cells. Therefore it is conceivable that postmitotic neurons, such as Purkinje cells react differently to continuous activation of the Akt pathway: loss of PTEN action on PI3K disinhibits growth factor signalling. Overexpression of Akt may confer hyper-responsiveness to ambient levels of growth factors, for example, by upregulation of insulin-like growth factor 1, which may render specific neuronal populations particularly sensitive to growth factors and Akt-mediated effects.

In two recent studies, *GFAP-Cre* mice were generated to inactivate *Pten* selectively in astrocytes. However, *GFAP-Cre*

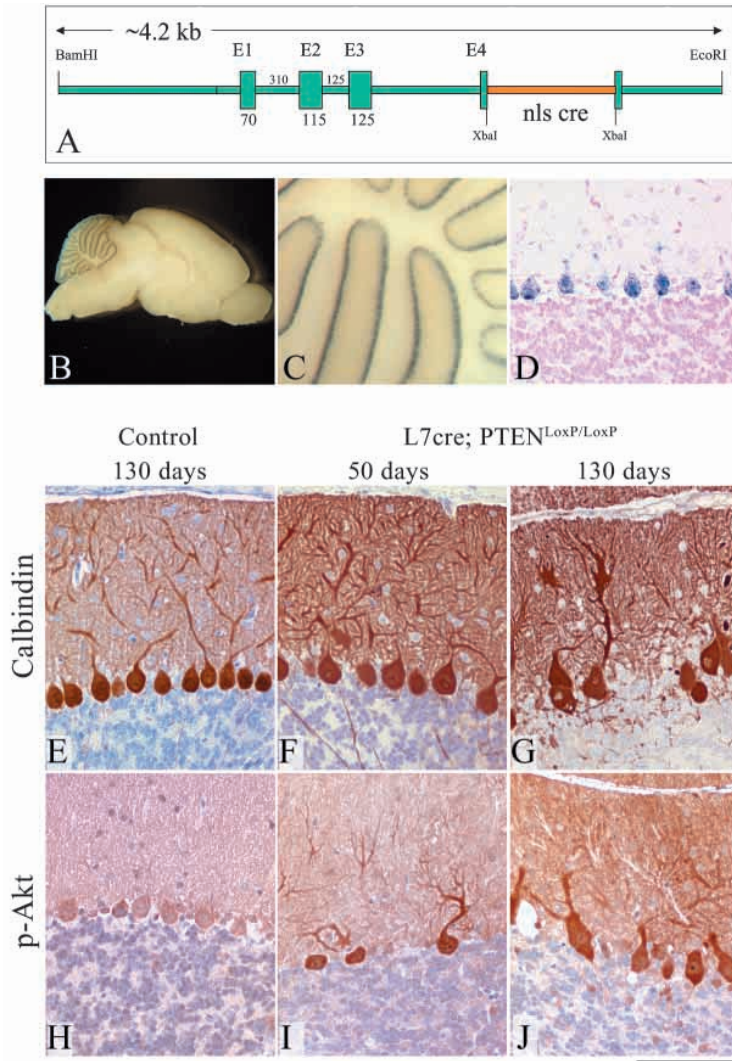


Fig. 7. Analysis of *L7cre*; *Pten^{LoxP/LoxP}* mice. (A) Transgenic construct used for microinjection. Whole-mount β -gal staining of Purkinje cells in *L7cre*; ROSA26R mouse brains (B,C) and after paraffin embedding and counterstaining with nuclear Fast Red (D). Calbindin immunostaining of wild-type (E), 7-week-old *L7cre*; *Pten^{LoxP/LoxP}* mice (F) and 16-week-old *L7cre*; *Pten^{LoxP/LoxP}* mice (G), showing increase of cell size with thickening of dendritic processes, vacuolisation, degeneration and progressive loss of Purkinje cells. Immunostaining for phosphorylated AKT (H-J) reveals baseline levels in Purkinje cells, Bergmann glia cells and Golgi cells in controls (H), while degenerating Purkinje cells of 7-week-old mice (I) and of 16-week-old mice (J) show heavy accumulation of p-AKT. Scale bar: 100 μ m in D-J.

was only expressed in a fraction of the astrocytes (Backman et al., 2001; Kwon et al., 2001), whereas *Pten* inactivation did occur in cerebellar and dentate gyrus granule cells and in some cortical neurons, presumably because of GFAP activity in neural precursor cells during development (Marino et al., 2000). In *En2cre*; *Pten^{LoxP/LoxP}* mice, we achieved inactivation of *Pten* during early embryonic development in precursor cells, giving rise to both glial and neuronal cell types. We show here for the first time that lack of *Pten* induces dysplasia in mature glial and neuronal cells. Dysplastic changes correlated with strong accumulation of p-Akt, indicating a possible

involvement of this pathway in cell dysplasia. Moreover, in contrast to previous findings (Backman et al., 2001; Kwon et al., 2001) we found a considerable p-Akt expression not only in *Pten*-deficient cells but already in Bergmann glia, Purkinje and Golgi cells of wild-type mice. These findings are supported by baseline p-Akt levels detected in western blots of vermis extracts of wild-type mice. Therefore the preferential involvement of glial and Purkinje cells in dysplasia and degeneration, respectively, might be explained by a further upregulation of an already active pathway.

Loss of heterozygosity for *PTEN* has been detected in many human cancers (Li et al., 1997; Podsypanina et al., 1999; Wang et al., 1997) and in line with these findings, mice chimaeric or heterozygous for *Pten* show an increased spontaneous tumour incidence (Di Cristofano et al., 1998). Inactivation of just one *Pten* allele has been shown to increase proliferation and cell survival and to decrease Akt and Parp dependent, Fas-mediated apoptosis in T- and B-lymphocytes (Di Cristofano et al., 1998). Therefore, *Pten* haploinsufficiency has been suggested to be an important factor in early selection and expansion of cells during transformation (Di Cristofano and Pandolfi, 2000). However, inactivation of one *Pten* allele during early CNS development in *En2cre* *Pten^{LoxP/+}* mice and in Purkinje cells of *L7cre*; *Pten^{LoxP/+}* mice failed to result in increases of cell size, deficits in migration and differentiation, dysplasia, or upregulation of p-Akt levels in *L7cre*; *Pten^{LoxP/+}* mice (Fig. 5), indicating that development and neoplastic transformation in the CNS are not affected by *Pten* gene dose. Moreover, we show that inactivation of both *Pten* alleles in the cerebellum is not sufficient to elicit neoplastic transformation. Hence, this points to a role of PTEN in late tumour progression and invasion, in agreement with previous studies on human tumours.

Both the mouse model presented here and the reports published previously (Backman et al., 2001; Kwon et al., 2001) suggest that malformations in Lhermitte-Duclos disease may originate from diverse cell populations affected by loss of *Pten* at different stages of development. As cerebellar malformations in Lhermitte-Duclos are a rather heterogeneous entity with high variability of morphological abnormalities, it is most likely that *Pten* inactivation in precursor cell populations during different stages of development gives rise to variable migration defects associated with increased thickness of foliation, or, in more extreme cases, disorganisation or loss of foliation. Our findings support the view of Kwon and co-workers (Kwon et al., 2001) and Backman and colleagues (Backman et al., 2001) that Lhermitte-Duclos disease is a hamartomatous lesion rather than a neoplastic proliferative disorder. Using this model, we provide further insight into the pathogenesis of CNS malformations associated with germline or somatic mutations of *Pten*.

We thank Marianne König, Beatrice Pfister and Mauri Peltola for excellent histological assistance, Thomas Rüllicke for the microinjection of the *L7cre* construct, and the staff of the Biologisches

Zentrallabor for animal caretaking. L7 promoter construct was a gift from Jim Morgan (St Jude Children's Research Hospital, Memphis, TN); *Math1* probe was obtained from H. Zoghbi (HHMI, Baylor College of Medicine, Houston, TX); and the *mGluR2* plasmid was received from Shigetada Nakanishi (Kyoto University, Japan). We are grateful to Alexandra Joyner (Skirball Institute of Biomolecular Medicine, New York University School of Medicine New York, NY) for providing us with the *Engrailed-2 cre* transgenic mice. The work was supported by a grant of the Schweizerischer Nationalfonds (31-64266.00) to S. M. and S. B., and by the Novartis Foundation to S. M.

REFERENCES

- Backman, S. A., Stambolic, V., Suzuki, A., Haight, J., Elia, A., Pretorius, J., Tsao, M. S., Shannon, P., Bolon, B., Ivy, G. O. et al. (2001). Deletion of Pten in mouse brain causes seizures, ataxia and defects in soma size resembling Lhermitte-Duclos disease. *Nat. Genet.* **29**, 396-403.
- Ben-Arie, N., Hassan, B. A., Bermingham, N. A., Malicki, D. M., Armstrong, D., Matzuk, M., Bellen, H. J. and Zoghbi, H. Y. (2000). Functional conservation of atonal and *Math1* in the CNS and PNS. *Development* **127**, 1039-1048.
- Benninger, Y., Marino, S., Hardegger, R., Weissmann, C., Aguzzi, A. and Brandner, S. (2000). Differentiation and histological analysis of embryonic stem cell-derived neural transplants in mice. *Brain Pathol.* **10**, 330-341.
- Cantley, L. C. and Neel, B. G. (1999). New insights into tumor suppression: PTEN suppresses tumor formation by restraining the phosphoinositide 3-kinase/AKT pathway. *Proc. Natl. Acad. Sci. USA* **96**, 4240-4245.
- Di Cristofano, A. and Pandolfi, P. P. (2000). The multiple roles of PTEN in tumor suppression. *Cell* **100**, 387-390.
- Di Cristofano, A., Pesce, B., Cordon-Cardo, C. and Pandolfi, P. P. (1998). Pten is essential for embryonic development and tumour suppression. *Nat. Genet.* **19**, 348-355.
- Di Cristofano, A., Kotsi, P., Peng, Y. F., Cordon-Cardo, C., Elkon, K. B. and Pandolfi, P. P. (1999). Impaired Fas response and autoimmunity in *Pten*^{-/-} mice. *Science* **285**, 2122-2125.
- Durand, B. and Raff, M. (2000). A cell-intrinsic timer that operates during oligodendrocyte development. *BioEssays* **22**, 64-71.
- Eves, E. M., Xiong, W., Bellacosa, A., Kennedy, S. G., Tschlis, P. N., Rosner, M. R. and Hay, N. (1998). Akt, a target of phosphatidylinositol 3-kinase, inhibits apoptosis in a differentiating neuronal cell line. *Mol. Cell. Biol.* **18**, 2143-2152.
- Gary, D. S. and Mattson, M. P. (2001). Integrin signaling via the PI3-kinase-Akt pathway increases neuronal resistance to glutamate-induced apoptosis. *J. Neurochem.* **76**, 1485-1496.
- Groszer, M., Erickson, R., Scripture-Adams, D., Lesche, R., Trumpp, A., Zack, J. A., Kornblum, H. I., Liu, X. and Wu, H. (2001). Negative regulation of neural stem/progenitor cell proliferation by the Pten tumor suppressor gene in vivo. *Science* **294**, 2186-2189.
- Helms, A. W. and Johnson, J. E. (1998). Progenitors of dorsal commissural interneurons are defined by MATH1 expression. *Development* **125**, 919-928.
- Jimenez, C., Portela, R. A., Mellado, M., Rodriguez-Frade, J. M., Collard, J., Serrano, A., Martinez, A. C., Avila, J. and Carrera, A. C. (2000). Role of the PI3K regulatory subunit in the control of actin organization and cell migration. *J. Cell Biol.* **151**, 249-262.
- Kwon, C. H., Zhu, X., Zhang, J., Knoop, L. L., Tharp, R., Smeyne, R. J., Eberhart, C. G., Burger, P. C. and Baker, S. J. (2001). Pten regulates neuronal soma size: a mouse model of Lhermitte-Duclos disease. *Nat. Genet.* **29**, 404-411.
- Lhermitte, J. and Duclos, P. (1920). sur un ganglioneurome diffuse du cortex du cervelet. *Bull. Assoc. Fran. Etude Cancer* **9**, 99-107.
- Li, J., Yen, C., Liaw, D., Podsypanina, K., Bose, S., Wang, S. I., Puc, J., Miliaresis, C., Rodgers, L., McCombie, R. et al. (1997). PTEN, a putative protein tyrosine phosphatase gene mutated in human brain, breast, and prostate cancer. *Science* **275**, 1943-1947.
- Lloyd, K. and Dennis, M. (1963). Cowden's disease: a possible new symptom complex with multiple system involvement. *Ann. Intern. Med.* **58**, 136-142.
- Marino, S., Vooijs, M., van Der Gulden, H., Jonkers, J. and Berns, A. (2000). Induction of medulloblastomas in p53-null mutant mice by somatic inactivation of Rb in the external granular layer cells of the cerebellum. *Genes Dev.* **14**, 994-1004.
- Marsh, D. J., Coulon, V., Lunetta, K. L., Rocca-Serra, P., Dahia, P. L., Zheng, Z., Liaw, D., Caron, S., Duboue, B., Lin, A. Y. et al. (1998a). Mutation spectrum and genotype-phenotype analyses in Cowden disease and Bannayan-Zonana syndrome, two hamartoma syndromes with germline PTEN mutation. *Hum. Mol. Genet.* **7**, 507-515.
- Marsh, D. J., Dahia, P. L., Caron, S., Kum, J. B., Frayling, I. M., Tomlinson, I. P., Hughes, K. S., Eeles, R. A., Hodgson, S. V., Munday, V. A. et al. (1998b). Germline PTEN mutations in Cowden syndrome-like families. *J. Med. Genet.* **35**, 881-885.
- Marsh, D. J., Kum, J. B., Lunetta, K. L., Bennett, M. J., Gorlin, R. J., Ahmed, S. F., Bodurtha, J., Crowe, C., Curtis, M. A., Dasouki, M. et al. (1999). PTEN mutation spectrum and genotype-phenotype correlations in Bannayan-Riley-Ruvalcaba syndrome suggest a single entity with Cowden syndrome. *Hum. Mol. Genet.* **8**, 1461-1472.
- Ming, G., Song, H., Berninger, B., Inagaki, N., Tessier-Lavigne, M. and Poo, M. (1999). Phospholipase C-gamma and phosphoinositide 3-kinase mediate cytoplasmic signaling in nerve growth cone guidance. *Neuron* **23**, 139-148.
- Miyazawa, K., Himi, T., Garcia, V., Yamagishi, H., Sato, S. and Ishizaki, Y. (2000). A role for p27/Kip1 in the control of cerebellar granule cell precursor proliferation. *J. Neurosci.* **20**, 5756-5763.
- Oberdick, J., Smeyne, R. J., Mann, J. R., Zackson, S. and Morgan, J. I. (1990). A promoter that drives transgene expression in cerebellar Purkinje and retinal bipolar neurons. *Science* **248**, 223-226.
- Ohishi, H., Shigemoto, R., Nakanishi, S. and Mizuno, N. (1993). Distribution of the mRNA for a metabotropic glutamate receptor (mGluR3) in the rat brain: an in situ hybridization study. *J. Comp. Neurol.* **335**, 252-266.
- Padberg, G. W., Schot, J. D., Vielvoye, G. J., Bots, G. T. and de Beer, F. C. (1991). Lhermitte-Duclos disease and Cowden disease: a single phakomatosis. *Ann. Neurol.* **29**, 517-523.
- Podsypanina, K., Ellenson, L. H., Nemes, A., Gu, J., Tamura, M., Yamada, K. M., Cordon-Cardo, C., Catoretti, G., Fisher, P. E. and Parsons, R. (1999). Mutation of Pten/Mmac1 in mice causes neoplasia in multiple organ systems. *Proc. Natl. Acad. Sci. USA* **96**, 1563-1568.
- Schwenk, F., Baron, U. and Rajewsky, K. (1995). A cre-transgenic mouse strain for the ubiquitous deletion of loxP-flanked gene segments including deletion in germ cells. *Nucleic Acids Res.* **23**, 5080-5081.
- Shen, T. L. and Guan, J. L. (2001). Differential regulation of cell migration and cell cycle progression by FAK complexes with Src, PI3K, Grb7 and Grb2 in focal contacts. *FEBS Lett.* **499**, 176-181.
- Soriano, P. (1999). Generalized lacZ expression with the ROSA26 Cre reporter strain. *Nat. Genet.* **21**, 70-71.
- Stambolic, V., Suzuki, A., de la Pompa, J. L., Brothers, G. M., Mirtsos, C., Sasaki, T., Ruland, J., Penninger, J. M., Siderovski, D. P. and Mak, T. W. (1998). Negative regulation of PKB/Akt-dependent cell survival by the tumor suppressor PTEN. *Cell* **95**, 29-39.
- Tamura, M., Gu, J., Matsumoto, K., Aota, S., Parsons, R. and Yamada, K. M. (1998). Inhibition of cell migration, spreading, and focal adhesions by tumor suppressor PTEN. *Science* **280**, 1614-1617.
- Tamura, M., Gu, J., Danen, E. H., Takino, T., Miyamoto, S. and Yamada, K. M. (1999a). PTEN interactions with focal adhesion kinase and suppression of the extracellular matrix-dependent phosphatidylinositol 3-kinase/Akt cell survival pathway. *J. Biol. Chem.* **274**, 20693-20703.
- Tamura, M., Gu, J., Takino, T. and Yamada, K. M. (1999b). Tumor suppressor PTEN inhibition of cell invasion, migration, and growth: differential involvement of focal adhesion kinase and p130Cas. *Cancer Res.* **59**, 442-449.
- Tanno, S., Mitsuuchi, Y., Altomare, D. A., Xiao, G. H. and Testa, J. R. (2001). AKT activation up-regulates insulin-like growth factor I receptor expression and promotes invasiveness of human pancreatic cancer cells. *Cancer Res.* **61**, 589-593.
- Wang, S. I., Puc, J., Li, J., Bruce, J. N., Cairns, P., Sidransky, D. and Parsons, R. (1997). Somatic mutations of PTEN in glioblastoma multiforme. *Cancer Res.* **57**, 4183-4186.
- Zhou, B. P., Liao, Y., Xia, W., Spohn, B., Lee, M. H. and Hung, M. C. (2001). Cytoplasmic localization of p21Cip1/WAF1 by Akt-induced phosphorylation in HER-2/neu-overexpressing cells. *Nat. Cell Biol.* **3**, 245-252.
- Zinyk, D. L., Mercer, E. H., Harris, E., Anderson, D. J. and Joyner, A. L. (1998). Fate mapping of the mouse midbrain-hindbrain constriction using a site-specific recombination system. *Curr. Biol.* **8**, 665-668.